Cellular Physiology and Biochemistry

Cell Physiol Biochem 2016;38:1085-1099

DOI: 10.1159/000443059
Published online: March 04, 2016

Accepted: February 10, 2016

1421-9778/16/0383-1085$39.50/0
www.karger.com/cpb

Original Paper

Characterization of Microvesicles Released from Human Red Blood Cells

Duc Bach Nguyen[a] Thi Bich Thuy Ly[b] Mauro Carlos Wesseling[c] Marius Hittinger[d] Afra Torge[e] Andrew Devitt[f] Yvonne Perrie[g] Ingolf Bernhardt[c]

[a]Department of Molecular Biology, Faculty of Biotechnology, Vietnam National University of Agriculture, Ngo Xuan Quang, Trau Quy, Gia Lam, Hanoi, [b]Institute of Biotechnology, Vietnam Academy of Science and Technology, Hanoi, Vietnam; [c]Laboratory of Biophysics, Faculty 8, Saarland University, Saarbruecken, [d]PharmBioTec GmbH, Saarbruecken, Germany and Helmholtz-Institute for Pharmaceutical Research Saarland, Saarbruecken, [e]Department of Pharmacy, Biopharmaceutics and Pharmaceutical Technology, Saarland University Saarbruecken, Germany; [f]School of Life & Health Sciences, Aston University, Aston Triangle, Birmingham, [g]Aston Pharmacy School, Aston University, Aston Triangle, Birmingham, UK

Key Words
Red blood cells • Microvesicles • Phosphatidylserine • Fluorescence imaging • Cell adhesion

Abstract
Background/Aims: Extracellular vesicles (EVs) are spherical fragments of cell membrane released from various cell types under physiological as well as pathological conditions. Based on their size and origin, EVs are classified as exosome, microvesicles (MVs) and apoptotic bodies. Recently, the release of MVs from human red blood cells (RBCs) under different conditions has been reported. MVs are released by outward budding and fission of the plasma membrane. However, the outward budding process itself, the release of MVs and the physical properties of these MVs have not been well investigated. The aim of this study is to investigate the formation process, isolation and characterization of MVs released from RBCs under conditions of stimulating Ca^{2+} uptake and activation of protein kinase C. ***Methods:*** Experiments were performed based on single cell fluorescence imaging, fluorescence activated cell sorter/flow cytometer (FACS), scanning electron microscopy (SEM), atomic force microscopy (AFM) and dynamic light scattering (DLS). The released MVs were collected by differential centrifugation and characterized in both their size and zeta potential. ***Results:*** Treatment of RBCs with 4-bromo-A23187 (positive control), lysophosphatidic acid (LPA), or phorbol-12 myristate-13 acetate (PMA) in the presence of 2 mM extracellular Ca^{2+} led to an alteration of cell volume and cell morphology. In stimulated RBCs, exposure of phosphatidylserine (PS) and formation of MVs were observed by using annexin V-FITC. The shedding of MVs was also observed in the case of PMA treatment in the absence of Ca^{2+}, especially under the transmitted bright field illumination. By using SEM, AFM and DLS the morphology and size of stimulated RBCs, MVs were characterized. The sizes of the two populations of MVs were 205.8 ± 51.4 nm and 125.6 ± 31.4 nm, respectively. Adhesion of stimulated RBCs and MVs was observed. The zeta potential

Duc Bach Nguyen

Department of Molecular Biology, Faculty of Biotechnology, Vietnam National University of Agriculture, Ngo Xuan Quang, Trau Quy, Gia Lam, Hanoi, (Vietnam)
Tel. +84 983 926497, E-Mail ndbach@vnua.edu.vn, E-Mail ndbach@gmail.com

of MVs was determined in the range from - 40 mV to - 10 mV depended on the solutions and buffers used. ***Conclusion:*** An increase of intracellular Ca^{2+} or an activation of protein kinase C leads to the formation and release of MVs in human RBCs.

Introduction

Under physiological as well as pathological conditions, various cell types release small spherical fragments called membrane vesicles or extracellular vesicles (EVs). So far many different terms for these EVs such as ectosomes, microvesicles (MVs), shedding vesicles, apoptosomes or microparticles have been used in a number of reports [1-5]. Recently, based on their size and origin of formation, EVs have been classified as exosomes, MVs and apoptotic bodies [6-10].

Exosomes are small enclosed membrane vesicles of nearly uniform size from 30 to 100 nm already described by Johnstone during the *in vitro* culture of sheep reticulocytes [11]. They were also observed in a variety of cultured cells such as lymphocytes, dendritic cells, cytotoxic T cells, mast cells, neurons, oligodendrocytes, Schwann cells, and intestinal epithelial cells [12, 13]. In these cells, exosomes originated from the endosomal network that locates within large sacs in cytoplasm. The release of exosomes to extracellular environment is carried out by the fusion of these sacs to the plasma membrane [7, 12, 14].

Distinct from exosomes, the biogenesis of MVs arises through direct outward budding and fission of the plasma membrane following different kinds of cell activation or during early state of apoptosis [15]. Normally, MVs are larger compared to exosomes with the size ranging from 50 to 1000 nm [15-17]. However, there is an overlapping of the size between exosomes and MVs. So far the mechanism of biogenesis is primarily used to distinguish MVs and exosomes [4, 6, 16]. The formation and release of MVs is the result of dynamic processes of phospholipid redistribution and cytoskeletal protein breakdown [6].

A vast amount of literature dealing with the release mechanism of MVs in RBCs and their properties in response to A23187, ATP depletion, oxidative stress and storage has been reported (e.g. [18-24]). In addition, an increase of the levels of RBC-derived MVs in the circulating blood of patients with sickle cell anemia (SCA), thalassemia and glucose-6-phosphate-deficiency (G6PD) has been observed [25, 26]. Morphological transitions of RBCs stimulated by exogenous compounds, according to the bilayer-couple hypothesis, also result in the formation of MVs [19, 22, 27]. Furthermore, the reorganization of the cell membrane such as loss of asymmetrical membrane phospholipid distribution leads to membrane blebbing and formation of MVs [28-31]. Recently, numbers of studies have shown that an increase of the intracellular Ca^{2+} concentration by opening Ca^{2+} channels or activation of protein kinase C (PKC) leads to PS exposure and formation of MVs in many different cell types including human RBCs [29, 30, 32, 33].

In contrast, apoptotic bodies have been characterized as largest EVs with the size varying from 1 to 5 μm. Nucleated cells undergoing apoptosis pass through several stages, beginning with condensation of the nuclear chromatin, followed by membrane blebbing, and finally releasing EVs and apoptotic bodies [6]. However apoptotic cells are also known to release smaller vesicles (MV) in response to apoptosis induction and these MVs are known to stimulate innate immune responses [34]. Although mature human RBCs have no nucleus and organelles, however, they are able to undergo an apoptosis-like process (also called eryptosis [28, 29]) with similar characteristics, e.g. membrane blebbing and formation of MVs [28, 29].

Although there is a number of reports about the formation of MVs in RBCs, investigations of the kinetics of this process as well the characterization of released MVs are still limited. By using different methods and techniques we investigated the kinetics of formation of MVs. In addition, the MVs released from human RBCs under different conditions were also isolated and characterized. The study may contribute for understanding the role of MVs in normal biological process and diseases.

Materials and Methods

Blood and solutions

Fresh human venous blood from healthy donors was obtained from the Institute of Sports and Preventive Medicine (Saarland University, Saarbruecken) and from the Institute of Clinical Haematology and Transfusion Medicine (Saarland University Hospital, Homburg). Blood was withdrawn by venipuncture into citrate-coated tubes or with heparin as anticoagulant, stored at 4°C and used within one day. Freshly whole blood was centrifuged at 2,000 g for 5 min at room temperature and the plasma and buffy coat was removed by aspiration. Subsequently, RBCs were washed 3 times in HEPES buffered physiological solution (HPS) containing (mM): NaCl 145, KCl 7.5, glucose 10, HEPES 10, pH 7.4. Finally, RBCs were re-suspended in HPS and kept at 4°C for experiments.

For experiments, RBCs were used at 0.05% haematocrit in HPS containing additionally 2 mM$CaCl_2$ and incubated with Ca^{2+} inonophore 4-bromo-A23187 (positive control, further abbreviated as A23187) or LPA or PMA. After 2 h incubation at 37°C cells were washed in HPS. The concentrations of A23187, LPA, and PMA chosen in the present study are in accordance with previous investigations showing an optimal effect [30, 35].

Kinetic study of the formation and release of microvesicles

The formation and shedding of MVs was investigated by using an inverted fluorescence microscope (Eclipse TE2000-E, Nikon, Tokyo, Japan) under both transmitted bright field illumination and fluorescence modes. The exposure of phosphatidylserine (PS) in the outer layer of the plasma membrane and in MVs can be displayed by annexin V-FITC with excitation and emission wavelength at 488 nm and 512 nm, respectively. RBCs were prepared in HPS in the presence of 2 mM $CaCl_2$and 5 µl of annexin V-FITC (0.05% haematocrit). The suspension was transferred to a cover slip (previously coated with poly-L-lysine 0.01%). When the cells were settled on the surface of the cover slip, an imaging procedure for the kinetics of MVs formation was recorded immediately after adding A23187 at final concentration of 2 µM or PMA at 6 µM. For experiment with LPA, the substance was added before the addition of Ca^{2+} (to avoid the influence of Ca^{2+} on the solubility of this moiety [36]). Experiments in the presence of A23187, LPA, or PMA were also carried out in the absence of extracellular Ca^{2+} by adding 2 mM EGTA. For controls, ethanol or DMSO was added.

To take into consideration a possible effect of the intracellular glutathione (GSH) level, bright field imaging experiments were performed with RBCs pre-incubated with N-Acetyl-L-Cysteine (NAC) for 1 h and then stimulated with PMA under 4 different conditions: without NAC, treated with NAC (1 mM), PMA, and NAC plus PMA. All these experiments were carried out in HPS with and without Ca^{2+}.

Our experimental approach was designed to provide a real-time assessment of the formation of MVs, while maintaining identical imaging parameters under all conditions. This was accomplished by taking images with an electron multiplication CCD camera (CCD97, Photometrics, Tucson, USA) using a 100×1.4 (NA) oil immersion lens with infinity corrected optics. An image was taken every 20 s for 120 min using the imaging software VisiView (Visitron Systems GmbH, Puchheim, Germany). Exposure time was 4000 ms for fluorescence and 100 ms for bright field transmitted light. Experiments were performed at room temperature in a dark room.

Stimulation of RBCs and isolation of MVs

RBCs were treated with LPA, PMA or A23187 as stated before for stimulating the formation of EVs. RBCs were suspended in HPS solution at 0.05% haematocrit in the presence of 2 mM $CaCl_2$. Subsequently, A23187 or LPA or PMA was added at concentrations of 2 µM, 2.5 µM or 6 µM, respectively (LPA was added before the addition of Ca^{2+}). After incubation for 2 h at 37°C with occasionally shaking, cell suspensions were subjected to differential centrifugation. First, a centrifugation step at 1,500 g for 10 min was applied followed by centrifugation at 3,000 g for 15 min twice to remove intact cells, cell debris, and apoptotic blebs. The supernatants were collected and further centrifuged at 25,000 g for 1 h at 4°C to harvest large size MVs. Subsequently, the collected supernatants were transferred to new tubes and ultra-centrifuged at 35,000 rpm (corresponding to about 200,000 g) for 2 h at 4°C for the isolation of small size MVs (Beckman Coulter, Swinging Bucket rotor SW40 Ti, k-factor 137).

To obtain all MVs, after removing intact cells, cell debris, and apoptotic blebs, the supernatants were directly subjected to ultra-centrifuge at 200,000 g for 2 h at 4ºC. Pellets obtained after each centrifugation step were re-suspended in Milli-Q water (ultra-pure) for morphological, size and zeta potential measurements.

Flow cytometry

Samples were analyzed using a FACScalibur Flow Cytometer (Becton Dickinson Biosciences, Franklin Lakes, USA) and BD CellQuest™ Pro Software 5.2.1. All acquisition and analysis were done using log mode. The parameters were set up using standard calibration kit (BD Calibrite™, BD Calibrite 3 Beads, BD Biosciences). Parameters of both forward and side scatter were adjusted to remove instrument noise (dust). The gating process was done by using a combination of sheath fluid (blank), samples of stimulated RBCs, isolated MVs stained with fluorescence dyes annexin V-FITC for PS and Dil as lipophilic tracer.

Morphological analysis using SEM and AFM

Stimulated RBCs under conditions mentioned above were fixed with 2% glutaraldehyde at room temperature for 10 min and washed in phosphate buffered saline, pH 7.4 (PBS-TWEEN® Tablets, 1 tablet per litre, Calbiochem - Merck, Darmstadt, Germany) by centrifugation at 5,000 g for 5 min at room temperature to remove glutaraldehyde. The pellets were re-suspended in Milli-Q water and immediately applied on glass slides and air-dried for 1 h. The slides were dipped quickly and gently washed stepwise with ethanol from 50, 70, 90 to 100% for dehydration. For SEM analysis, the prepared slides were sputtered with a gold layer of 15 nm thickness prior to SEM imaging (Sputter coater: Quorum Q150R ES, Quorum Technologies Ltd, East Grinstead, UK) and kept in a closed box at room temperature.

To prepare samples of MVs for SEM analysis, these particles were fixed with 2% glutaraldehyde for 10 min at room temperature. Subsequently the samples were washed in phosphate buffered saline by an ultra-centrifuge step at 200,000 g for 30 min at 4°C. Further steps were performed similar to the preparation of stimulated RBCs described above.

For SEM imaging (EVO HD15, Carl Zeiss Microscopy GmbH, Jena, Germany), several randomly selected frames from each sample were captured for morphological observation and statistical purpose. SEM imaging was carried out using 5 kV acceleration voltage and secondary electron (SE) detector.

AFM equipment (Bioscope IV, Veeco Instruments, Santa Barbara, USA) was used for topographical imaging. Glutaraldehyde-fixed samples of stimulated RBCs, MVs were scanned in air by tapping-mode. The cantilever OMCL-AC160TS series (Olympus) was used with nominal spring constant of 26 N/m, tip radius less than 10 nm and reflective side coated with Al. Data of height, amplitude and phase modes were recorded simultaneously. The images were scanned at the resolution of 256 × 256 pixels, scanning rate in the range from 0.3 to 0.75 Hz. Topographical images were analyzed and displayed using NanoScope Analysis 1.5 software (Brucker Corporation).

Size and zeta potential measurement

A Zetasizer Nano ZS (Malvern, Worcestershire, UK) was used for MVs size and zeta potential measurement. Uniform polystyrene particles of 100, 200 and 400 nm diameter (Bangs Laboratories, Fishers, USA) at 001% in phosphate buffered saline (PBS) were used to verify instrument operation. For size measurement, the MVs samples were diluted in Milli-Q water (attenuator index position in the range from 7 to 9) and analyzed using the standard operation procedure (SOP) as follows: sample refractive index 1.43 (phospholipid liposomes), dispersant refractive index 1,33 (water), system temperature at 25°C and sample equilibration time for 60 s. One ml of each sample was measured in disposable polystyrene (DTS0012, Malvern Instruments) with a path length of 10 mm. Observed populations of particles were characterized by associated Z-average size (nm) and polydispersity index (PdI).

For zeta potential measurement, the disposable capillary cell DTS1070 (Malvern Instruments) was used. Samples were measured in different solutions and buffers: Milli-Q water, NaCl 5 mM or 10 mM, and Tris-HCl 5 mM or 10 mM, pH 7.0. The SOP was set up similar as described above. Each sample was measured 3 times with maximum 100 runs in automatic mode. Observed populations of particles were characterized by associated phase (rad) and zeta potential (mV).

The Malvern Zetasizer software v7.03 was used to collect and analyze the data. The error bars displayed on the DLS graphs were presented by the standard deviation (SD) of three measurements of the same sample.

Reagents

A23187, LPA, PMA and NAC were purchased from Sigma-Aldrich (St. Louis, USA). Annexin V-FITC and Dil stain (DiIC18(3)) were obtained from Life Technologies (Carlsbad, USA). In this study, A23187 was

dissolved in absolute ethanol at 1 mM. LPA and PMA were dissolved in DMSO at 1 mM and stored at -20°C. NAC was prepared as 0.5 M stock solution in water placed in a heating block for 1 h. Glutaraldehyde (for electron microscopy), and all other chemicals were at analytical grade and purchased from Sigma-Aldrich.

Statistics

Data are presented as the mean values ± S.D. of at least 3 experiments of different blood samples. Statistical analysis was performed using Student's t-test when Gaussian distributed. The values were taken as significant difference when $p \leq 0.05$ or $p \leq 0.01$. Otherwise, a Mann-Whitney test was performed.

Results

Kinetic formation of microvesicles

It has been shown that treatment of human RBCs with A23187, LPA, or PMA in the presence of extracellular Ca^{2+} leads to an increase of intracellular Ca^{2+} and exposure of PS in the outer cell membrane leaflet [30, 32, 37]. In our recent publication we mentioned that after treatment of human RBCs with these substances MVs have been observed [30]. However, this observation was not in the focus of that paper. Therefore, in this paper we investigated the process of membrane blebbing and formation of MVs and characterized these particles in more detail. Figure 1 shows the kinetics of the formation and the outward budding process of MVs in human RBCs after stimulation with A23187, LPA or PMA. The lag time before the formation of MVs started was different among different substances used for stimulation.

Treatment with A23187 resulted in a reduction of cell volume already after 5 min (not shown but can be seen in [30, 35]). The formation of MVs can be clearly seen after 15 min (small spots on the surface of RBCs and in the solution). The MVs were formed and subsequently released into the medium. The exposure of PS can be observed also after 15 min. After 2 h almost all cells show PS exposure and MVs on the cell membrane (Fig. 1, upper row).

In case of LPA treatment, after 10 min, there was an alteration in the morphology of RBCs from the echinocyte or discocyte to a spherical shape (not shown). Subsequently, MVs begin to appear on the cell surface. Although the process of PS exposure on the outer leaflet

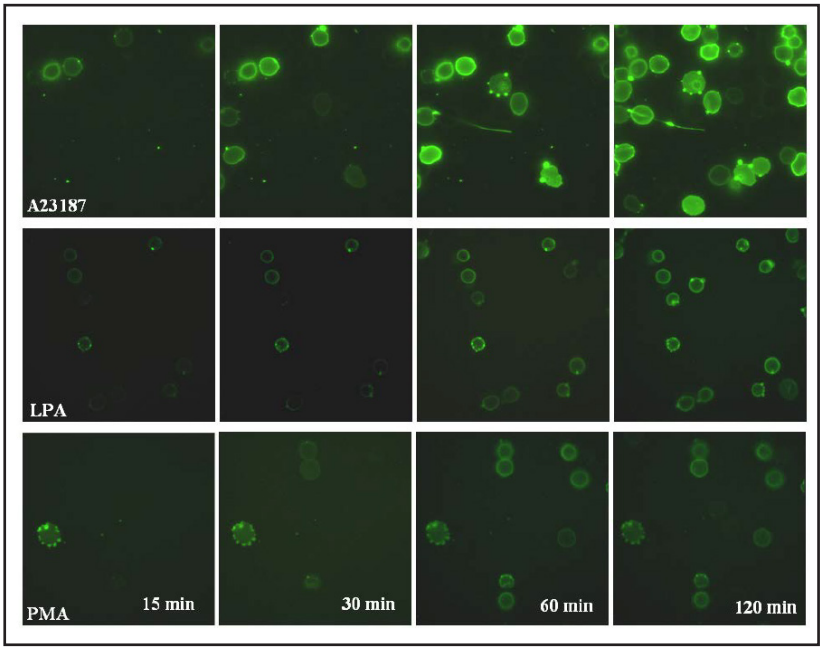

Fig. 1. Fluorescence imaging of the formation of MVs in human RBCs depending on time (up to 120 min) stimulated with 2 µM A23187 (upper row), 2.5 µM LPA (middle row) and 6 µM PMA (lower row) in the presence of 2 mM $CaCl_2$. Annexin V-FITC has been used for PS staining. The images of time zero (0 min) were not presented because of the completely absence of fluorescence signal. One typical experiment out of 10 is shown.

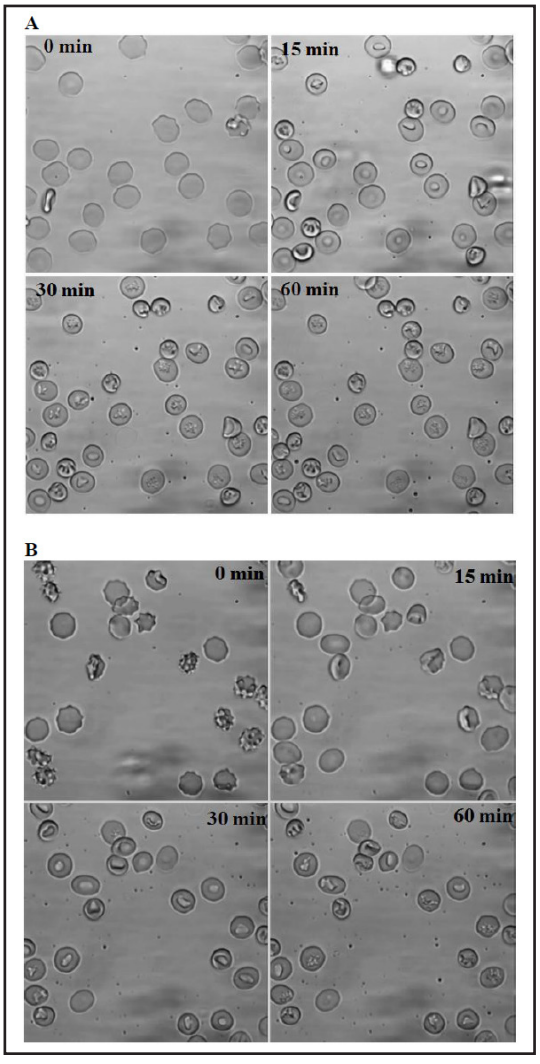

Fig. 2. Bright field imaging of the formation of MVs in human RBCs depending on time (up to 60 min) stimulated by 6 µM PMA in the absence of $CaCl_2$ (with 2 mM EGTA) (A) or in the presence of 2 mM $CaCl_2$ (B). One typical experiment out of 6 is shown.

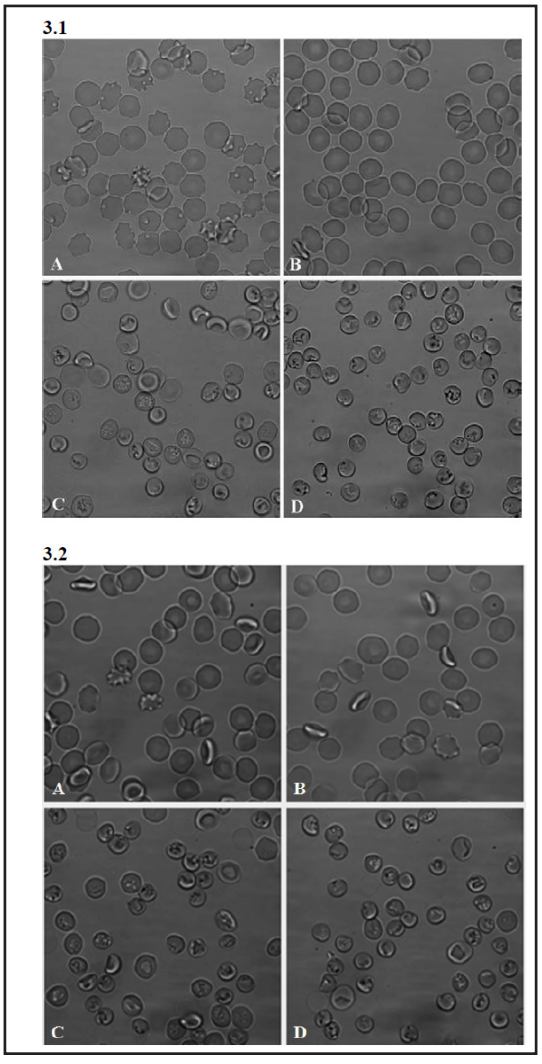

Fig. 3. Bright field imaging of the shape and the formation of MVs in human RBCs in the absence of $CaCl_2$ (with 2 mM EGTA) (Fig. 3.1) or in the presence of 2 mM $CaCl_2$ (Fig. 3.2). A: RBCs in HPS without NAC; B: RBCs treated with 1 mM NAC for 1 h; C: RBCs treated with 6 µM PMA in the absence of NAC for 1 h; D: RBCs treated with 6 µM PMA and 1 mM NAC for 1 h. One typical experiment out of 3 is shown.

of cell membrane was faster in comparison to the case of A23187 treatment, the number of cells showing a positive annexin V- FITC signal was about 60% of the cells only (Fig. 1, middle row).

In the presence of PMA, RBCs with echinocyte or discocyte shape showed a tendency to change their morphology to stomatocytes after 10 min of treatment. The stomatocyte shape was unchanged over time and coupled with the formation and shedding of MVs (Figs. 2 and 3.1) after 15 min of treatment. The exposure of PS in the outer leaflet of the cell membrane could be observed in about 70% of the cells after 2 h of treatment (Fig. 1, lower row).

Under all experimental conditions, the exposure of PS in the outer cell membrane leaflet and the formation of MVs were observed. However, the fluorescence signal of annexin V-FITC in case of PMA is significant lower in comparison to LPA or A23187 (Fig. 1).

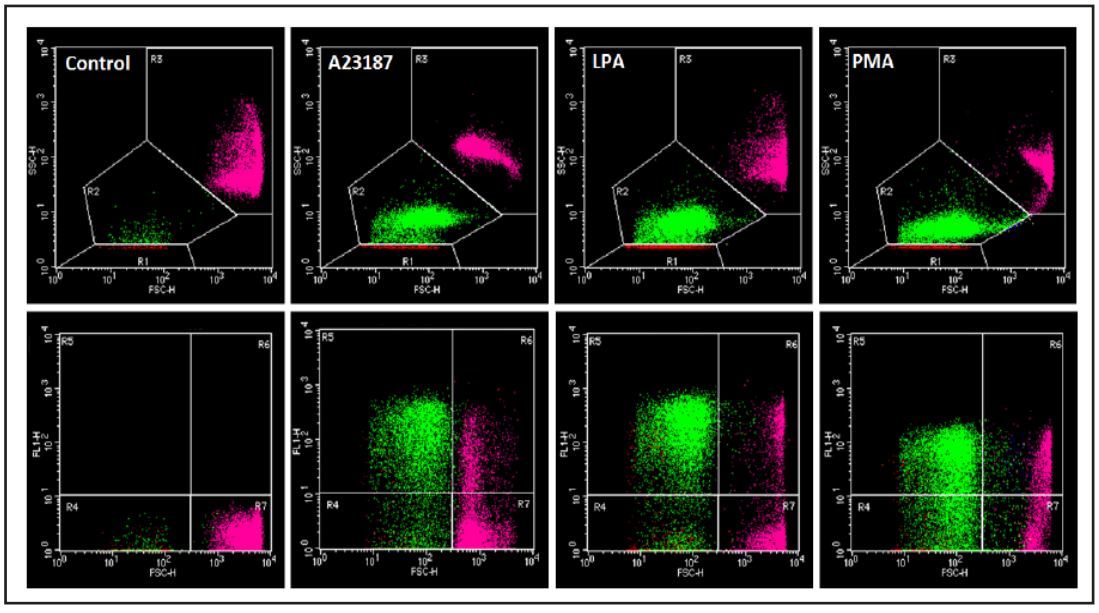

Fig. 4. Flow cytometry analysis of stimulated RBCs stained with annexin V-FITC. RBCs were stimulated with A23187, LPA or PMA for 2 h. The dot plots display the characteristics of the RBCs and MVs, the SSC *vs.* FSC (upper row) and the FL1 *vs.* FSC (lower row). Gates R1: instrument noise; R2: MVs and exosomes; R3: intact RBCs; R4: negative populations of small particles, MVs and exosomes; R5: positive population of MVs and exosomes; R6: positive population of RBCs; R7: negative population of RBCs.

Fluorescence imaging using annexin V-FITC for PS staining (Fig. 1) showed that under all stimulating conditions (A23187, LPA, PMA) only a small but more or less identical amount of MVs could be observed. However under bright-field imaging much more MVs can be seen in case of PMA treatment compared to fluorescence imaging (cp. Figs. 1, 2B) and compared to bright field imaging of cells and MVs after A23187 and LPA treatments (not shown). Furthermore, with bright field imaging, the formation of MVs was also clearly observed when RBCs were treated with PMA in the absence of Ca^{2+} (Fig. 2A).

Treatment of RBCs with NAC (1 mM) did not lead to changes of cell morphology in the presence or absence of extracellular Ca^{2+} (Fig. 3.1 A, B and Fig. 3.2 A, B). In addition, no significant difference in cell morphology between PMA-treated and NAC- plus PMA-treated cells in the presence or absence of extracellular Ca^{2+} could be observed (Fig. 3.1 C, D and Fig. 3.2 C, D). In all cases no significant differences in the formation of MVs were seen. There was also no PS exposure when RBCs were treated with NAC (data not shown).

Flow cytometry analysis

The formation of MVs was also analyzed by flow cytometry. In the controls (freshly washed RBCs) only a very small amount of MVs was observed (Fig. 4). For stimulated RBCs, the distribution of MVs was gated in R2 regions (Fig. 4). There was an overlapping of MVs with instrument noise but this was not significant. By staining with annexin V-FITC, the fractions of MVs showing PS on the outer surface were clearly separated from the noise. In addition, the fluorescent dye Dil was applied to stain MVs, RBCs and all particles derived from cell membrane. By using Dil, based on its lipophilic properties, we were able to separate RBCs, MVs, and instrument noise due to the high fluorescence signal of Dil bound to phospholipid components (Fig. 5).

All released MVs from stimulated RBCs were analyzed by flow cytometer (Fig. 6). The FSC *vs.* SSC dot plots displayed the distribution of MVs in the region R2. By staining with annexin V-FITC almost all MVs showed PS on their surfaces (gate R5). In case of LPA stimulation, more than 85% MVs showed positive signal of annexin V-FITC and about 15%

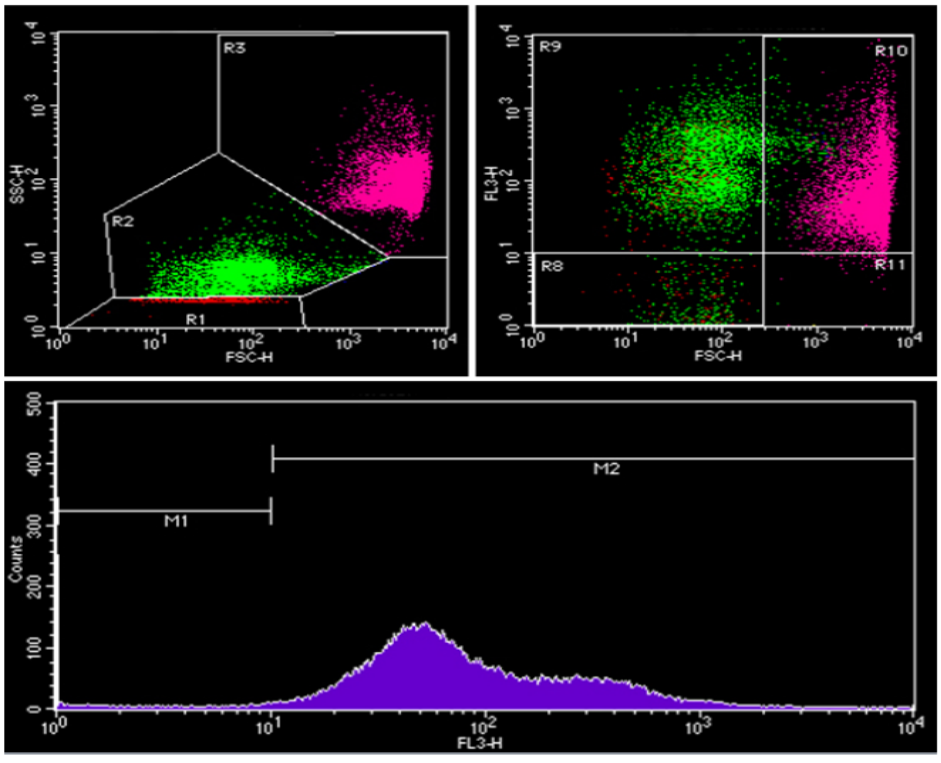

Fig. 5. Flow cytometry analysis of stimulated RBCs stained with the fluorescent dye Dil. The dot plots display the characteristics of the stimulated RBCs with LPA for 2 h. The SSC *vs.* FSC (upper left) and the FL3 *vs.* FSC (upper right); instrument noise (R1); MVs and exosomes (R2); intact RBCs (R3); population of MVs and exosomes showing negative signal and instrument noise (R8); population of MVs and exosomes showing positive signal (R9); population of stimulated RBCs showing positive signal (R10); population of RBCs showing negative signal (R11); In histogram (lower), population of MVs and exosomes showing negative signal and instrument noise (M1); population of simulated RBCs, MVs and exosomes showing positive signal with Dil (M2).

of MVs displayed no signal (gate R4). In all experiments, instrument noise was accounted for less than 1% of all detected events.

Particle size and zeta potential analysis

After removing intact cells, cell debris and apoptotic bodies, all MVs released from stimulated RBCs were collected by centrifugation at 200,000 g for 2 h at 4°C. DLS analysis showed that the size of released particles was very heterologous (PDI = 1.0). A symmetric multimodal distribution of particles in the range from 70 to 1000 nm with the mean value of about 200 nm was observed (Fig. 7A).

The population of larger particles (MVs) obtained by centrifugation at 25,000 g for 1 h (see Materials and methods) has sizes from 150 nm to 300 nm (Fig. 7B). The mean value of the size of MVs from 3 different measurements was 205.8 ± 51.4 nm. After collecting MVs, the population of MVs with smaller size was obtained by a further step of ultracentrifugation at 200,000 g for 2 h. DLS data showed that the size of these small MVs was 125.6 ± 31.4 nm (Fig. 7C). There was an overlapping in the size of two populations in the region from 150 to 200 nm (Fig. 7B and C) Under the experimental conditions, no significant difference was observed in the size distribution of MVs released from RBCs stimulated by LPA, PMA or A23187.

Under experimental conditions, MVs are negatively charged (Fig. 8). There was no significant difference in the charge between the populations of MVs. Data analysis showed

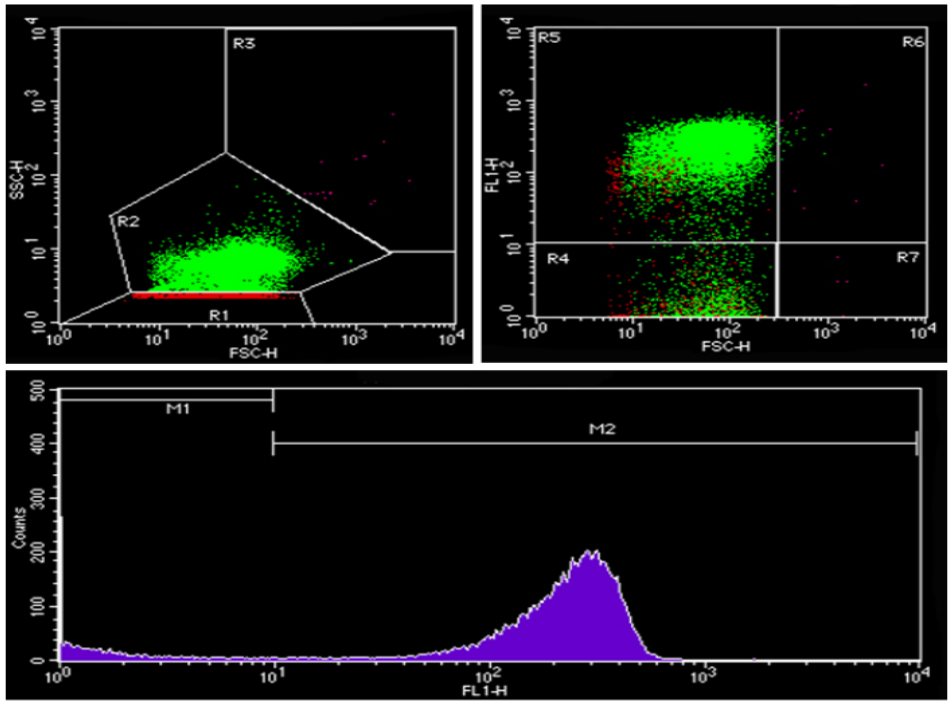

Fig. 6. Isolated MVs from RBCs stimulated by LPA for 2 h. The dot plots display the characteristics of the RBCs and MVs, the SSC *vs.* FSC (left) and the FL1 *vs.* FSC (right). Gates R1: instrument noise; R2: MVs and exosomes; R3: intact RBCs; R4: negative populations of small particles (MVs, exosomes, noise); R5: positive population of MVs and exosomes; R6: positive population of RBCs; R7: negative population of RBCs. Histogram shows the number of events with positive signal of annexin V-FITC (M2); events with negative signal and instrument noise (M1).

that the charge of MVs depend on the concentration of ions and the pH of solutions or buffers ($p < 0.01$). No significant difference in the charge of MVs released from RBCs stimulated by A23187 and LPA was observed (Fig. 8). However, there was a slight difference in the charge of MVs released from RBCs stimulated by PMA in comparison to those released after LPA or A23187 treatment ($p < 0.05$) when they were measured in Milli-Q water. Under all stimulating conditions, the lowest negative charge of MVs was determined of approximately -40 mV in Milli-Q water (Fig. 8). In case of phosphate saline buffer, the zeta potential values of MVs were recorded of about -10 mV, however, no distribution curve was observed (data not shown).

Particle morphological analysis

The morphology and size of stimulated RBCs, MVs were analyzed by SEM (Fig. 9). In comparison to control (RBCs in PBS), the morphology of stimulated RBCs was altered. The formation of MVs has been observed on the surface of stimulated RBCs. In addition, an adhesion of stimulated RBCs was clearly observed (Fig. 9 A1, A2, B1, B2 and C). Under all stimulating conditions, released MVs showed spherical shape and high polydispersity in their size. Statistical analysis showed that the size of MVs is in the range from 100 to 300 nm with the average value of about 200 nm (Fig. 9 E and F).

The size and morphology of MVs were also analyzed by AFM technique using tapping-mode. Data analysis from height, amplitude and phage modes showed that the size of these particles varied from about 70 to 200 nm (Fig. 10). There was no significant difference in size and morphology of MVs released from stimulated RBCs using PMA, LPA or A23187. In addition, the adhesion of MVs was observed in all samples.

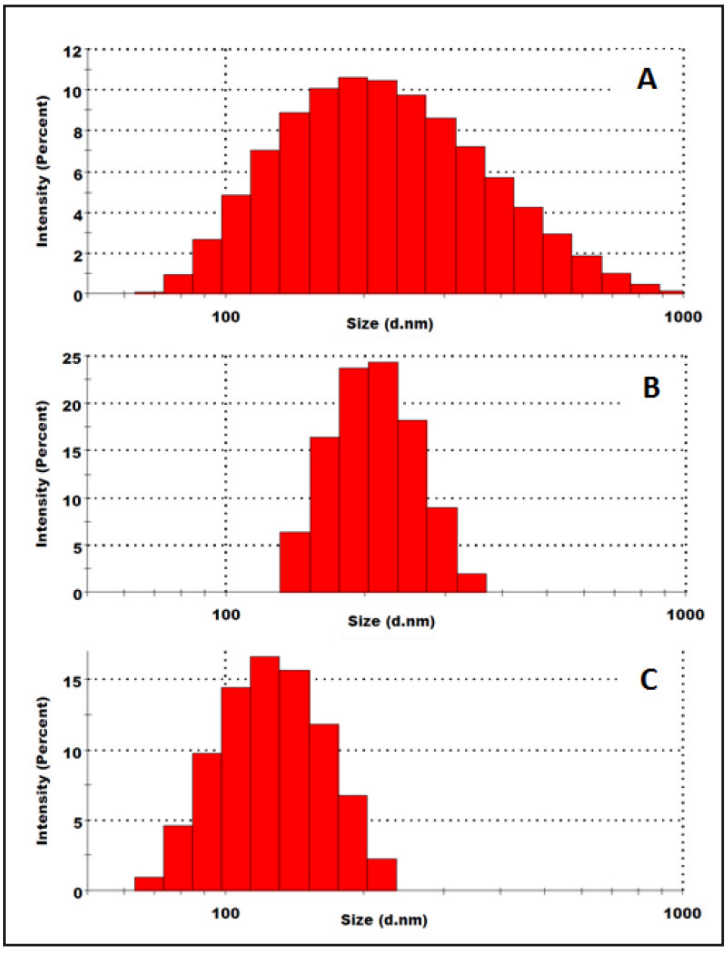

Fig. 7. Size distribution (d – diameter, in nm) of intensity of MVs and exosomes from RBCs stimulated with PMA. Symmetric multimodal distribution of all particles including MVs and exosomes (A), population of MVs (B) and population of exosomes (C).

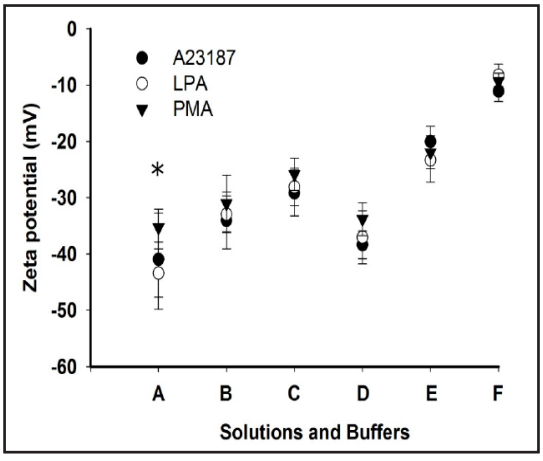

Fig. 8. Zeta potential distribution of MVs released from stimulated RBCs. Different solutions and buffers were used to measure zeta potential, Milli-Q water (A); NaCl 5 mM, pH 7.0 (B); NaCl 15 mM, pH 7.0 (C); Tris-HCl 5 mM, pH 7.0 (D); Tris-HCl 15 mM, pH 7.0 (E); Phosphate buffered saline, pH 7.4 (F). MVs released from RBCs stimulated with A23187 (●); MVs released from RBCs stimulated with LPA (○); MVs released from RBCs stimulated with PMA (▼). Error bars represent S.D. from 3 different experiments. In Mili-Q water, a significant difference in the charge of MVs released from RBCs stimulated by PMA was shown in comparison to LPA and A23187 (Student's t-test, $p < 0.05$(*)).

Discussion

Already 5 - 10 min after stimulation of RBCs with LPA, PMA or A23187 changes of cell volume and cell morphology were observed. In addition, exposure of PS on the outer cell membrane leaflet together with the formation and shedding of MVs were clearly seen on the surface of the cells by staining with annexin V-FITC. There was a relation between the exposure of PS and the formation of MVs. In the population of MVs released from RBCs stimulated by A23187 and LPA, the number of MVs showing positive signal for annexin

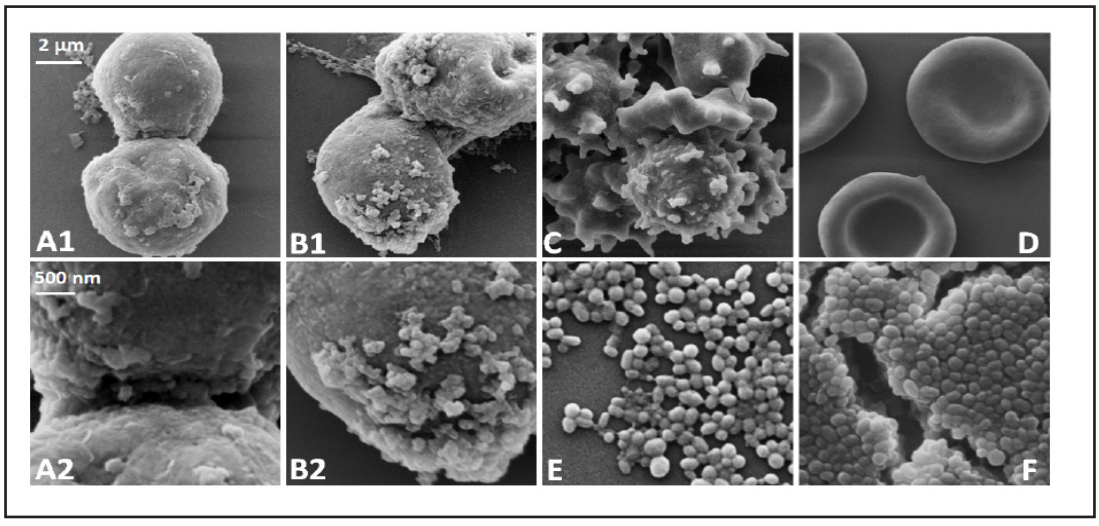

Fig. 9. SEM analysis of stimulated RBCs, released MVs and exosomes. Upper row: RBCs stimulated with PMA (A1); LPA (B1) or A23187 (C); RBCs in PBS/control (D). Lower row: Magnification of the binding area of two RBCs stimulated with PMA (A2); formation of MVs on the surface of RBCs stimulated with LPA (B2); MVs isolated from RBCs stimulated with PMA (E); large stack of MVs adhered together (F). The scale bars of 2 µm and 500 nm are applied for images in the upper row and lower row, respectively.

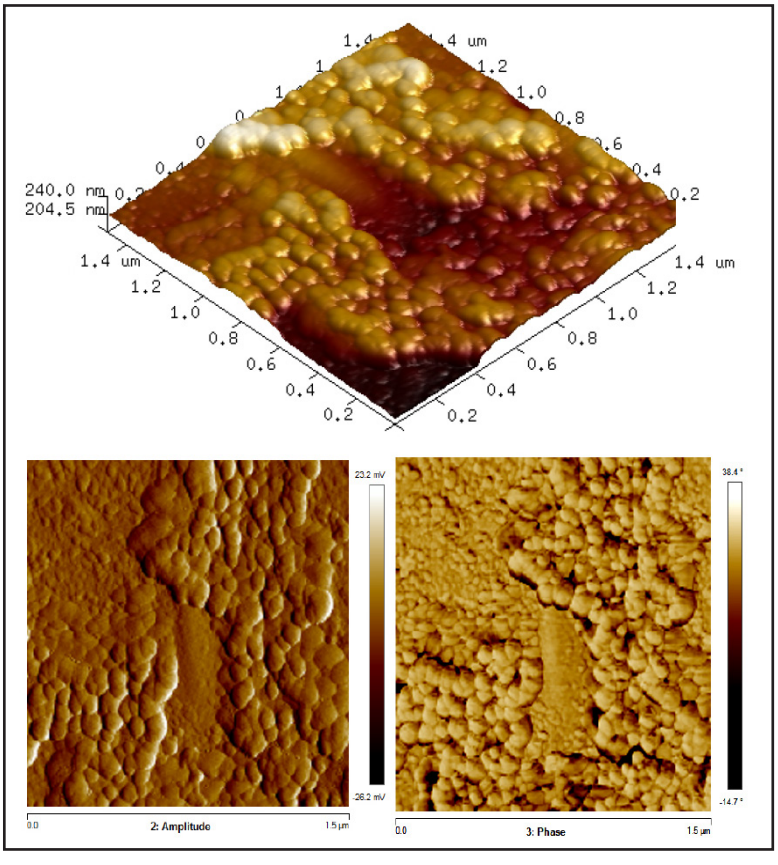

Fig. 10. Tapping-mode image of glutaraldehyde-fixed MVs and exosomes released from RBCs stimulated with LPA. Overview scan (1.5 × 1.5 µm) of a typical sample, height mode (upper), amplitude mode (lower left) and phase mode (lower right).

V-FITC was accounted for about 85%. In case of PMA, the number of MVs with positive signal was only about 60% (see gates R4 and R5 of Fig. 4). By comparison the obtained data from MVs stained with annexin V-FITC and Dil, a lipophilic tracer, it revealed that not all MVs showed PS in their outer surface (Fig. 5).

So far, the mechanism for the exposure of PS and shedding of MVs in human RBCs have been described by sustained elevation of intracellular calcium [30, 38-40] and other events associated with Ca^{2+} such as the opening of the Gardos channel leading to K^+ efflux, accompanied by an Cl^- efflux, and subsequently to a water efflux and reduction of cell volume [41]; activation of the scramblase [42, 43]; activation of calcium-dependent proteases, including calpain [17, 44, 45]; cytoskeletal alterations [46, 47] and change in erythrocyte morphology from the normal discoid shape to a spherical shape [48]. However, in case of PMA, the formation and shedding of MVs occurs in both Ca^{2+}-dependent and -independent ways (Figs. 2 and 3.1). The results suggest that this process is not only affected by Ca^{2+}-dependent parameters. Other pathways, e.g., the activation of protein kinase C, could also play a substantial role [30, 33]. However, a direct physical effect of PMA due to partitioning in the cell membrane on annexin V-FITC binding and releasing of MVs cannot be ruled out completely.

NAC has been reported as a thiol-oxidizing agent which is able to decrease the level of intracellular GSH in RBCs [49] and finally leading to the formation of MVs in G6PD deficient RBCs [50]. However, in the present study we show that treatment of RBCs from healthy people with NAC in the absence of PMA does not result in any changes of cell morphology and formation of MVs (Figs. 3.1 and 3.2). In the presence of PMA, the morphology of RBCs changed from echinocytes or discocytes to stomatocytes coupled with the release of MVs. However, there was no significant difference between RBCs treated with only PMA and both NAC and PMA (Figs. 3.1 and 3.2). It suggests that the effect of oxidative stress caused by the reduction of GSH level is not sufficient to stimulate the formation of MVs within the time-course of the experiment.

At the moment, it is unclear whether the MVs are formed and shed randomly or only in certain regions of the plasma membrane [3, 6]. If this process takes place randomly, in principle, the phospholipid components and membrane proteins in MVs will be comparable with the plasma membrane. Therefore, the regions of plasma membrane of RBCs showing PS on the outer leaflet may be a part of all MVs. However, as mentioned above, there was a subpopulation of MVs showing no PS on their outer layer. This suggests that in the whole population of MVs there exist different types of MVs carrying different components of phospholipids and probably membrane proteins on their surfaces. By differential centrifugation, the population of MVs at different size can be partly separated. However, these particles should be clearly separated based on other criteria rather than merely based on their size. However, so far efficient and specific markers to distinguish populations of MVs released from human RBCs have not been described [6, 51].

The negative charge of MVs can be explained based on the negative charged PS on the outer layer of MVs [17, 52]. Therefore, the negative charge of MVs depends on the number of PS on their outer layer. In addition, the adhesion of MVs themselves and RBCs carrying MVs should be clarified (Fig. 9). Since MVs have a negative surface charge they will repel each other and spread apart. However, Ca^{2+}could play an intermediate role forming molecular cross-bridges among MVs or stimulated RBCs showing PS on their surfaces. In this case it is not easy to explain the adhesion of stimulated RBC with PMA in the absence of Ca^{2+} [35]. In order to explain this adhesion, the involvement of receptors and adhesion proteins should be taken into account [4, 8, 17, 35]. Based on these findings, one could suggest that the exposure of PS in the outer cell membrane leaflet and the release of MVs may be directly involved in the aggregation of RBCs during thrombus formation as well as the RBC clearance by macrophages under normal physiological conditions or at certain diseases [37, 53, 54].

Conclusion

Treatment of RBCs with LPA, PMA or A23187 in the presence of Ca^{2+} led to the exposure of PS on the outer cell membrane leaflet and the release of MVs. A similar effect was seen in RBCs when protein kinase C was activated. The exposure of PS was observed in almost

all MVs. However, there was a subpopulation of these particles, which did not show PS on their outer layers. The size of released MVs varied from 70 to 1000 nm. By differential centrifugation, two populations of MVs were separated with size of 205.8 ± 51.4 nm and 125.6 ± 31.4 nm, respectively. All population of MVs revealed a negative charge of about - 40 mV in Milli-Q water. Adhesion among MVs and simulated RBCs was also observed. These findings suggest that the MVs may be involved in blood clot formation and the RBC clearance by macrophages.

Acknowledgements

This research is funded by Vietnam National Foundation for Science and Technology Development (NAFOSTED) under grant number 106-YS.06-2013.16 and Researcher Links Travel Grant from British Council. MCW is supported by a grant from CNPq (Brasil).

Disclosure Statement

The authors declare no conflict of interest.

References

1 Holme PA., Solum NO, Brosstad, F, Roger M, Abdelnoor M: Demonstration of platelet-derived microvesicles in blood from patients with activated coagulation and fibrinolysis using a filtration technique and western blotting. Thromb Haemost 1994;72:666-671.
2 Hess C, Sadallah S, Hefti A, Landmann R, Schifferli JA: Ectosomes released by human neutrophils are specialized functional units. J Immunol 1999;163:4564-4573.
3 Cocucci E, Racchetti G, Meldolesi J: Shedding microvesicles: artefacts no more. Trends Cell Biol 2009;19:43-51.
4 Gyorgy B, Szabo TG, Pasztoi M, Pal Z, Misjak P, Aradi B, Laszlo V, Pallinger E, Pap E, Kittel A, Nagy G, Falus A, BuzasEI: Membrane vesicles, current state-of-the-art: emerging role of extracellular vesicles. Cell Mol Life Sci 2011;68:2667-2688.
5 Trams, EG, Lauter C J, Salem N, Jr Heine U: Exfoliation of membrane ecto-enzymes in the form of micro-vesicles. Biochim Biophys Acta 1981;645, 63-70.
6 Akers J C, Gonda D, Kim R, Carter BS, Chen CC: Biogenesis of extracellular vesicles (EV): exosomes, microvesicles, retrovirus-like vesicles, and apoptotic bodies. J Neurooncol 2013;113:1-11.
7 Raposo G, Stoorvogel W: Extracellular vesicles: exosomes, microvesicles, and friends, J Cell Biol 2013;200:373-383.
8 Colombo M, Raposo G, Thery C: Biogenesis, secretion, and intercellular interactions of exosomes and other extracellular vesicles. Annu Rev Cell DevBiol 2014;30:255-289.
9 Comelli L, Rocchiccioli S, Smirni S, Salvetti A, Signore G, Citti L, Trivella, MG, Cecchettini A: Characterization of secreted vesicles from vascular smooth muscle cells. Mol Biosyst 2014;10:1146-1152.
10 Crescitelli R, Lasser C, Szabo TG, Kittel A, Eldh M, Dianzani I, BuzasEI, Lotvall J: Distinct RNA profiles in subpopulations of extracellular vesicles: apoptotic bodies, microvesicles and exosomes. J Extracell Vesicles 2013;2:20677- http://dx.doi.org/10.3402/jev.v2i0.20677.
11 Johnstone RM, Adam M, Hammond JR, Orr L, Turbide C: Vesicle formation during reticulocyte maturation. Association of plasma membrane activities with released vesicles (exosomes). J Biol Chem 1987;262:9412-9420.
12 Simons M, Raposo G: Exosomes-vesicular carriers for intercellular communication. Curr Opin Cell Biol 2009;21:575-581.
13 Thery C, Boussac M, Veron P, Ricciardi-Castagnoli P, Raposo G, Garin J, Amigorena S: Proteomic analysis of dendritic cell-derived exosomes: a secreted subcellular compartment distinct from apoptotic vesicles. J Immunol 2001;166:7309-7318.

14 Thery C, Ostrowski M, Segura E: Membrane vesicles as conveyors of immune responses. Nat Rev Immunol 2009;9:581-593.
15 Inal JM, Kosgodage U, Azam S, Stratton D, Antwi-Baffour S, Lange S: Blood/plasma secretome and microvesicles. Biochim Biophys Acta 2013;1834:2317-2325.
16 Muralidharan-Chari V, Clancy JW, Sedgwick A, D'Souza-Schorey C: Microvesicles: mediators of extracellular communication during cancer progression. J Cell Sci 2010;123:1603-1611.
17 Tissot J.-D, Canellini G, Rubin O, Angelillo-Scherrer A, Delobel J, Prudent M, Lion N: Blood microvesicles: From proteomics to physiology. Translat Proteom 2013;1:38-52.
18 Allan, D, Billah MM, Finean JB, Michell RH: Release of diacylglycerol-enriched vesicles from erythrocytes with increased intracellular (Ca2+). Nature 1976;261:58-60.
19 Allan D, Hagelberg C, Kallen KJ, Haest CW: Echinocytosis and microvesiculation of human erythrocytes induced by insertion of merocyanine 540 into the outer membrane leaflet. Biochim Biophys Acta 1989;986:115-122.
20 Allan D, Thomas P: Ca2+-induced biochemical changes in human erythrocytes and their relation to microvesiculation. J BioChem 1981;198:433-440.
21 Allan D, Thomas P, Limbrick AR: The isolation and characterization of 60 nm vesicles ('nanovesicles') produced during ionophore A23187-induced budding of human erythrocytes. J Bio Chem 1980;188:881-887.
22 Minetti G, Egee S, Morsdorf D, Steffen P, Makhro A, Achilli C, Ciana A, Wang J, Bouyer G, Bernhardt I, Wagner C, Thomas S, Bogdanova A, Kaestner L: Red cell investigations: art and artefacts. Blood Rev 213;27:91-101.
23 Lutz HU, Bogdanova A: Mechanisms tagging senescent red blood cells for clearance in healthy humans. Front Physiol 2013;4:387(doi: 10.3389/fphys.2013.00387).
24 Lutz HU, Liu SC, Palek J: Release of spectrin-free vesicles from human erythrocytes during ATP depletion. I. Characterization of spectrin-free vesicles. J Cell Biol 1977;73: 548-560.
25 Alaarg A, Schiffelers RM, van Solinge WW, van Wijk R: Red blood cell vesiculation in hereditary hemolytic anemia. Front Physiol 2013;4:365 (doi: 10.3389/fphys.2013.00365).
26 Camus SM, De Moraes JA, Bonnin P, Abbyad P, Le Jeune S, Lionnet F, Loufrani L, Grimaud L, Lambry JC, Charue D, Kiger L, Renard JM, Larroque C, Le Clésiau H, Tedgui A, Bruneval P, Barja-Fidalgo C, Alexandrou A, Tharaux PL, Boulanger CM, Blanc-Brude OP: Circulating cell membrane microparticles transfer heme to endothelial cells and trigger vasoocclusions in sickle cell disease. Blood 125;24:3805-3814.
27 Sheetz MP, Singer SJ: Biological membranes as bilayer couples. A molecular mechanism of drug-erythrocyte interactions. Proc Natl Acad Sci USA 1974;71:4457-4461.
28 Lang F, Gulbins E, Lerche H, Huber SM, Kempe DS, Foller M: Eryptosis, a window to systemic disease. Cell Physiol Biochem 2008;22:373-380.
29 Foller M, Huber SM, Lang F: Erythrocyte programmed cell death, IUBMB Life 2008;60:661-668.
30 Nguyen DB, Wagner-Britz L, Maia S, Steffen P, Wagner C, Kaestner L, Bernhardt I: Regulation of Phosphatidylserine Exposure in Red Blood Cells, Cell Physiol Biochem 2011;28:847-856.
31 Frasch SC, Henson PM, Kailey JM, Richter DA, Janes MS, Fadok VA, Bratton DL: Regulation of phospholipid scramblase activity during apoptosis and cell activation by protein kinase C delta. J BiolChem 2000;275:23065-23073.
32 Kaestner L, Steffen P, Nguyen DB, Wang J, Wagner-Britz L, Jung A, Wagner C. Bernhardt I: Lysophosphatidic acid induced red blood cell aggregation in vitro. Bioelectrochemistry 2012;87:89-95.
33 Wagner-Britz L, Wang J, Kaestner L, Bernhardt I: Protein kinase C alpha and P-type Ca channel CaV2.1 in red blood cell calcium signaling. Cell Physiol Biochem 2013;31:883-891.
34 Torr EE, Gardner DH, Thomas L, GoodallDM, Bielemeier A, Willetts R, Griffiths HR, Marshall LJ, Devitt A: Apoptotic cell-derived ICAM-3 promotes both macrophage chemoattraction to and tethering of apoptotic cells. Cell Death Differ 2012;19:671-679.
35 Steffen P, Jung A, Nguyen DB, Müller T, Bernhardt I, Kaestner L, Wagner C: Stimulation of human red blood cells leads to Ca2+-mediated intercellular adhesion. Cell Calcium 2011;50:54-61.
36 Pilpel Y, Segal M: The role of LPA1 in formation of synapses among cultured hippocampal neurons. J Neurochem 2006;97:1379-1392.
37 Chung SM, Bae ON, Lim KM, Noh JY, Lee MY, Jung YS, Chung JH: Lysophosphatidic acid induces thrombogenic activity through phosphatidylserine exposure and procoagulantmicrovesicle generation in human erythrocytes. Arterioscler Thromb Vasc Biol 2007;27:414-421.

38 Williamson P, Kulick A, Zachowski A, Schlegel RA, Devaux PF: Ca2+ induces transbilayer redistribution of all major phospholipids in human erythrocytes. Biochemistry 1992;31:6355-6360.
39 Bucki R, Bachelot-Loza C, Zachowski A, Giraud F, SulpiceJC: Calcium induces phospholipid redistribution and microvesicle release in human erythrocyte membranes by independent pathways. Biochemistry 1998;37:15383-15391.
40 KoshiarRL, Somajo S, Norstrom E, Dahlback B. Erythrocyte-derived microparticles supporting activated protein C-mediated regulation of blood coagulation. PLoS One 2014;9:e104200.
41 Lang PA, Kaiser S, Myssina S, Wieder T, Lang F, Huber SM: Role of Ca2+-activated K+ channels in human erythrocyte apoptosis. Am J Physiol Cell Physiol 2003;285:C1553-C1560.
42 Sahu SK, GummadiSN, Manoj N, AradhyamGK: Phospholipid scramblases: an overview. Arch Biochem Biophys 2007;462:103-114.
43 Basse F, Stout JG, Sims PJ, Wiedmer T: Isolation of an erythrocyte membrane protein that mediates Ca2+-dependent transbilayer movement of phospholipid. J Biol Chem 1996;271:17205-17210.
44 Berg CP, Engels IH, Rothbart A, Lauber K, Renz A, Schlosser SF, Schulze-Osthoff K, Wesselborg S: Human mature red blood cells express caspase-3 and caspase-8, but are devoid of mitochondrial regulators of apoptosis. Cell Death Differ 2001;8:1197-1206.
45 Tissot JD, Rubin O, Canellini G: Analysis and clinical relevance of microparticles from red blood cells. Curr Opin Hematol 2010;17:571-577.
46 Liu F, Mizukami H, Sarnaik S, Ostafin A: Calcium-dependent human erythrocyte cytoskeleton stability analysis through atomic force microscopy. J Struct Biol 2005;150:200-210.
47 Takakuwa Y: Protein 4.1, a multifunctional protein of the erythrocyte membrane skeleton: structure and functions in erythrocytes and nonerythroid cells. Int J Hematol 2000;72:298-309.
48 Gonzalez LJ, Gibbons E, Bailey RW, Fairbourn J, Nguyen T, Smith SK, Best KB, Nelson J, Judd AM, Bell JD: The influence of membrane physical properties on microvesicle release in human erythrocytes. PMC Biophys 2009;2:7 (doi:10.1186/1757-5036-2-7).
49 Kosower NS, Kosower EM, Wertheim B: Diamide, a new reagent for the intracellular oxidation of glutathione to the disulfide. Biochem Biophys Res Commun 1969;37:593-596.
50 Pantaleo A, Ferru E, Carta F, Mannu F, Simula LF, Khadjavi A, Pippia P, Turrini F: Irreversible AE1 tyrosine phosphorylation leads to membrane vesiculation in G6PD deficient red cells. PLoS One 2011;6:e15847.
51 Park JO, Choi DY, Choi DS, Kim HJ, Kang JW, Jung JH, Lee JH, Kim J, Freeman MR, Lee KY, GhoYS, KimKP: Identification and characterization of proteins isolated from microvesicles derived from human lung cancer pleural effusions. Proteomics 2013;13:2125-2134.
52 Rautou PE, Mackman N: Microvesicles as risk markers for venous thrombosis. Expert Rev Hematol 2013;6:91-101.
53 Andrews DA, Low PS: Role of red blood cells in thrombosis. Curr Opin Hematol 1999;6:76-82.
54 Bevers EM, WiedmerT, Comfurius P, Shattil SJ, Weiss HJ, Zwaal RF, Sims PJ: Defective Ca2+-induced microvesiculation and deficient expression of procoagulant activity in erythrocytes from a patient with a bleeding disorder: a study of the red blood cells of Scott syndrome. Blood 1992;79:380-388.